

Accepted Manuscript

Title: Development of multifunctional lipid nanocapsules for the co-delivery of paclitaxel and CpG-ODN in the treatment of glioblastoma.

Author: Giovanna Lollo Marie Vincent Gabriela
Ullio-Gamboa Laurent Lemaire Florence Franconi Dominique
Couez Jean-Pierre Benoit

PII: S0378-5173(15)30260-X
DOI: <http://dx.doi.org/doi:10.1016/j.ijpharm.2015.09.062>
Reference: IJP 15247

To appear in: *International Journal of Pharmaceutics*

Received date: 4-8-2015
Revised date: 23-9-2015
Accepted date: 26-9-2015

Please cite this article as: Lollo, Giovanna, Vincent, Marie, Ullio-Gamboa, Gabriela, Lemaire, Laurent, Franconi, Florence, Couez, Dominique, Benoit, Jean-Pierre, Development of multifunctional lipid nanocapsules for the co-delivery of paclitaxel and CpG-ODN in the treatment of glioblastoma. *International Journal of Pharmaceutics* <http://dx.doi.org/10.1016/j.ijpharm.2015.09.062>

This is a PDF file of an unedited manuscript that has been accepted for publication. As a service to our customers we are providing this early version of the manuscript. The manuscript will undergo copyediting, typesetting, and review of the resulting proof before it is published in its final form. Please note that during the production process errors may be discovered which could affect the content, and all legal disclaimers that apply to the journal pertain.

Development of multifunctional lipid nanocapsules for the co-delivery of paclitaxel and CpG-ODN in the treatment of glioblastoma.

Giovanna Lollo^{1,2}, Marie Vincent^{1,3,4}, Gabriela Ullio-Gamboa^{1,2}, Laurent Lemaire^{1,2}, Florence Franconi⁵, Dominique Couez^{1,3,4}, Jean-Pierre Benoit^{1,2*}

¹LUNAM Université — Micro et Nanomédecines Biomimétiques, F-49933 Angers, France

²INSERM U1066, IBS-CHU, 4 rue Larrey, F-49933 Angers Cedex 9, France

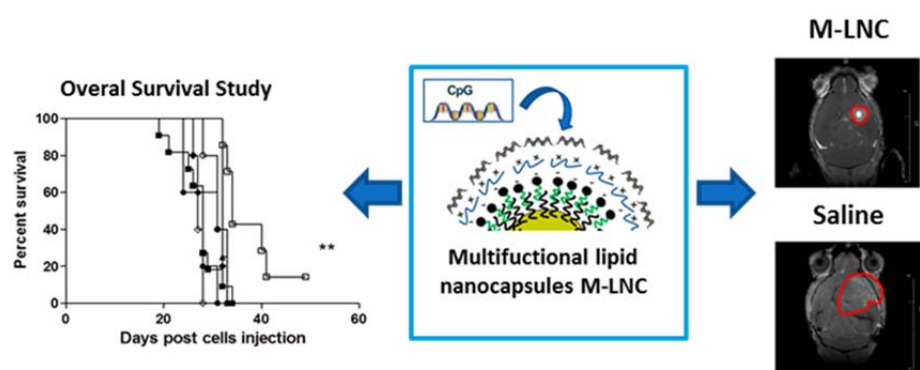
³INSERM, UMR892, F-49933 Angers, France

⁴CNRS, UMR 6299, F-49933 Angers, France

⁵PRIMEX-CIFAB, Université d'Angers, LUNAM Université, IRIS-IBS, CHU Angers F-49933 Angers, France

*Corresponding author.

Graphical Abstract



Abstract

In this work, multifunctional lipid nanocapsules (M-LNC) were designed to combine the activity of the cytotoxic drug paclitaxel (PTX) with the immunostimulant CpG. This nanosystem, consisting of modified lipid nanocapsules coated with a cationic polymeric shell composed of chitosan (CS), was able to allocate the hydrophobic drug PTX in the inner oily core, and to associate onto the surface the genetic material CpG. The CS-coated LNC (CS-LNC), showed a narrow size distribution with an average size of 70nm and a positive zeta potential (+25mV). They encapsulated PTX in a high amount (98%), and, due to the cationic surface charge, were able to adsorb CpG without losing stability. As a preliminary *in vitro* study, the apoptotic effect on GL261 glioma cells was investigated. The drug-loaded CS-LNC exhibited the ability to interact with glioma cells and induce an important apoptotic effect in comparison with blank systems. Finally, the M-LNC made of CS-LNC loaded with both CpG and PTX were tested *in vivo*, injected via Convection Enhanced Delivery (CED) in GL261-glioma-bearing mice. The results showed that the overall survival of mice treated with the M-LNC was significantly increased in comparison with the control, Taxol®, or the separated injection of PTX-loaded LNC and CpG. This effect was also confirmed by Magnetic Resonance Imaging (MRI) which revealed the reduction of tumor growth in the animals treated with CpG and PTX-loaded M-LNC. All these findings suggested that the developed M-LNC could potentiate both CpG immunopotency and PTX antitumor activity by enhancing its delivery into the tumor microenvironment.

Keywords: Nanotechnology; Lipid Nanocapsules; Antitumor drugs; Paclitaxel; CpG; Glioblastoma

1. Introduction

Over the last years the elucidation of the role of the immune system in cancer has opened new frontiers for the design of novel treatments. Cancer immunotherapy represents an attractive alternative that broadly aims to harness and redirect the patient's own immune system to recognize and fight tumors with high specificity (Reardon et al., 2013). This strategy is of particular interest for patients suffering from primary or secondary glioblastoma. Indeed, conventional therapy which includes surgery when possible, followed by radiation and chemotherapy, is non-specific and often results in crippling damage to healthy brain tissue. (Carter M Suryadevara, 2015; Finocchiaro and Pellegatta, 2011; Finocchiaro G, 2014). Glioblastomas exhibit a complex, immunosuppressive environment that suppresses endogenous antitumor immune-reactivity and fosters immune tolerance (Jarry et al., 2014). To reverse this effect, different approaches have been explored. The use of microbial moieties such as pathogen-associated molecular patterns or PAMPs, have demonstrated to promote immune-mediated tumor rejection through the stimulation of microglia cells (Andaloussi et al., 2006; Grauer et al., 2007; Grauer et al., 2008). Microglia, the innate immune cells which serve as a resident macrophage population in the brain, express Toll-like receptors (TLRs) and respond to TLR ligands producing pro-inflammatory molecules (Rivest, 2009). Among different TLR ligands, synthetic non-methylated oligonucleotides such as CpG have recently emerged as a powerful immunostimulator for both innate and specific immunity. CpG, a TLR9 ligand expressed by most murine immune cells, can trigger immune rejection and induce long-term immunity against gliomas (Ursu and Carpentier, 2012). However, CpG as a single intratumoral (i.t.) injection has also been studied in patients with recurrent gliomas with tolerable toxicity and partial tumor response in a few patients (Carpentier et al., 2010). One of the reasons of these treatment failures could be related to the low glioblastoma-cellular internalization of CpG following intratumoral administration (Badie B. 2013). Once injected, CpG needs to be taken up by immune cells in order to initiate the immune stimulation cascade. Moreover, CpG can be transported away from the site of injection and interact with both desired immune cells associated with healthy tissue, thus limiting its therapeutic efficacy (Badie B., 2013).

In this study, our working hypothesis was that by combining chemotherapy and the immune-stimulant agent in a single multifunctional delivery system may provide a more efficient treatment strategy

avoiding long time relapses, and enhancing the targeting of both active molecules. To this aim, paclitaxel (PTX) was selected as the drug model. Paclitaxel primarily exerts its effect on tumor cells by binding to the β -tubulin subunit in microtubules, preventing depolymerization and increasing their stability and rigidity. In addition, it was shown to stimulate innate and acquired immune responses (Buchanan et al., 2010; Javeed et al., 2009; Zitvogel et al., 2008). Our group has already developed PTX-loaded LNC which have been tested in a 9L orthotopic rat glioblastoma model (Garcion et al., 2006). Moreover, these nanocapsules were functionalized with a peptide in order to increase their uptake by the glioma cells (Balzeau et al., 2013). The results showed that encapsulation within the nanocapsules protect the drug from the surrounding medium and allows a sustained concentration of the drug and peptides at the tumour site, even after a single injection.

Based on these previous results, here we have developed a multifunctional nanosystem (M-LNC) adapted for the co-delivery of PTX and CpG. To this purpose, PTX-loaded LNC were modified with a cationic polymer, chitosan (CS), in order to functionalize them with CpG.

The goal was to assess the antitumor efficacy of the nanocarrier obtained, following stereotactic injection in GL261glioma-bearing mice, to show the potential of a synergistic effect between chemotherapy and immunotherapy.

2. Materials and Methods

Lipoid® S75-3 (soybean lecithin at 69% of phosphatidylcholine), Captex® 8000 (glyceryltricaprylate) and Solutol® HS15 (polyethyleneglycol ester of 12-hydroxystearic acid and polyethylene glycol-PEG-SA) were obtained from Lipoid GmbH (Ludwigshafen, Germany), Abitec Corp (Columbus, OH, USA) and BASF (Ludwigshafen, Germany), respectively. Ethanol Solution 96% was purchased from Fisher Scientific (Illkirch, France). Taxol® 6mg/ml solution and PTX powder were supplied by Bristol-Myers Squibb (Rueil-Malmaison, France) and LC Laboratories® (Woburn, MA 01801, USA), respectively. Sodium chloride, sodium dodecyl sulphate (SDS), chitosan low molecular weight (average Mn 5,000 Da, > 90% deacetylated), propidium iodide, bis-chloroethylnitrosourea (BCNU) and gel loading buffer were purchased from Sigma Aldrich (Saint-Quentin-Fallavier, France). CpG-ODN: Phosphorothioated-CpG-oligodeoxynucleotide 1826, seq (5'-3': tccatgacgttctctgacgtt) (CpG)

was purchased from Invivogen (Toulouse, France). Annexin V-FITC was purchased from BD Pharmingen (San Diego, CA, USA).

2.1 Development of blank and PTX-loaded LNC

The formulation of LNC was based on the phase inversion process described by Heurtault *et al.* (Heurtault B, 2002). LNC were composed of an oily core of lipophilic chains (Captex[®] 8000, 1.2g), lecithin (Lipoid[®] S75-3, 67.2mg), PEG-SA (Solutol[®] HS-15, 1g) in NaCl (73.3mg) and 1.8ml of water. Briefly, all the components were mixed together under magnetic stirring. Three temperature cycles were carried out to reach the phase-inversion from an oil-in-water to a water-in-oil emulsion. After, the mixture underwent a fast cooling-dilution process by adding 11.2ml of Milli-Q water which led to the formation of LNC. To obtain PTX-loaded LNC, 15mg PTX were first solubilized in 1ml of ethanol and Captex[®] 8000, and then all the other components were added (Groo AC, 2013). Once obtained, the nanocapsule suspension was filtered with 0.22 μ m Ministar[®] high flow filters (Sartorius, Aubagne, France) to remove the non-encapsulated drugs prior to HPLC quantification.

2.2 Design and development of PTX-loaded CS-LNC

CS-LNC were obtained following electrostatic layer by layer deposition of the cationic polymer on the negative surface of the LNCs. The negative charge of the LNCs arises from the presence of SDS surfactant which was added to the initial emulsion of LNC. In order to avoid the formation of SDS micelles, all the concentrations tested were below the CMC of this surfactant (8mM). Then, once the LNC with SDS were obtained, an aliquot of the suspension (1ml) was incubated with 0.5ml of CS solution (concentrations from 0 to 5mg/ml) and maintained under magnetic stirring at room temperature for 1h.

2.3 Physico-chemical characterization of LNC

The size distribution and surface charge of the prepared nanocarriers were analysed using a Malvern Zetasizer NanoSerie DTS 1060 (Malvern Instruments S.A., Worcestershire, UK). Sample suspensions were diluted in deionized water to ensure a convenient scatter intensity on the detector. The average

hydrodynamic diameter, the polydispersity index and the zeta potential were determined at 25°C in triplicate. The total amount of PTX was measured in triplicate experiments, destroying the LNC with ACN. The free drug was quantified following separation of the LNC by filtration with 0.22µm filter. In fact, the drug encapsulated, PTX, is a very hydrophobic compound and when it is not encapsulated, it precipitates in the LNC dispersion. If there is some precipitate, filtration through 0.22µm filter would ensure its elimination.

The aliquots of both no-filtrated and filtrated LNC were then treated with ANC and the following equation was used to calculate the encapsulation efficiency:

$$\text{E.E. (\%)} = (\text{B} \times 100) / \text{A}$$

Where A is the experimental total drug concentration and B is the drug concentration measured in the filtrated solution.

The determined amount of LNC dispersions was dissolved in a 96:4 (v/v) methanol/tetrahydrofuran mixture and a Waters Alliance 2690 HPLC system was used (Waters S.A., Saint-Quentin en Yvelines, France) to quantify the drug.

A 20µl aliquot of the filtrate was injected in triplicate into an HPLC XTerra RP18 column (5µm, 4.6mm×150mm) (Waters, Guyancourt, France). The analysis was performed with water and acetonitrile in the mobile phase, with a gradient elution program of 50–80% acetonitrile, at a flow rate of 1ml/min. Eluting fractions were revealed with a Waters 2487 Dual-absorbance Detector, at a wavelength of 227nm. Data were analyzed by the Empower Pro® software, version 5.00. PTX gave a retention peak at 7.2 minutes.

2.4 CpG association to PTX-loaded CS-LNC

To obtain the M-LNC, CpG was adsorbed on the surface of CS-LNC at 0.8-0.75-0.5 and 0.25% w/w loadings, defined as the percentage between the mass of CpG and the total mass of the formulation. For the adsorption procedure, the CpG solution (20µl, concentration 10 µg/ml) was added to the LNC suspension (80µl) and maintained under magnetic stirring for one hour to achieve an optimal interaction between the CpG and the nanocapsules. Different weight ratios were obtained by

modifying the concentration of CpG; meanwhile the concentration of nanocapsules was maintained constant. CpG-associated LNC were characterized according to size and zeta potential as detailed previously. Additionally, the association of CpG to the LNCs was studied by a conventional agarose gel electrophoresis assay. In order to displace the CpG adsorbed in the nanocapsules, an excess of heparin solution (15mg/ml-2.8 μ l) was added to the suspension and the mixture was incubated for 2 hours at 37°C (Lozano et al., 2013). The CpG was stained with SYBR® Green I by adding 2 μ l of the reagent diluted 1:50,000 in DMSO, to 100 μ l of the CpG-associated nanocapsules and 9 μ l of gel loading, and left to interact for 15 minutes. Then, the samples and the control of free CpG were loaded in 1.4 % agarose gel and run for 60 minutes at 50V in a TAE buffer (Sub-Cell GT 96/192, Bio-Rad Laboratories Ltd., Marnes-la-Coquette, France).

2.5 Stability of PTX-loaded CS-LNC

The stability of PTX-loaded CS-LNC was evaluated under storage conditions for one month at 4°C. Three sets of parameters were assessed at different time points: (i) macroscopic aspect (presence of aggregated, cream formation, changes in color); (ii) particle size, polydispersity and zeta potential; (iii) PTX concentration in the preparation and encapsulation efficiency. All these characteristics were determined as described above.

2.6 Cell line

The GL-261 murine glioma cell line (C57BL/6 origin, H2b), kindly provided by Dr Paul Walker (Geneva, Switzerland), was cultured in DMEM medium containing 10% heat-inactivated Fetal Calf Serum (FCS), 2mM glutamine, 10mM HEPES and 1mM sodium pyruvate (all from Lonza, Basel, Switzerland). The cell line was grown at 37°C under a humidified, 5% CO₂ atmosphere.

2.6.1 Cell apoptosis assay

The GL261 cell line was incubated with 500 μ M BCNU for 24 hours with different concentrations of Taxol®, PTX-loaded CS-LNC, and the corresponding blank formulation. The M-LNC, consisting of CpG-PTX-loaded CS-LNC, were also tested. Apoptotic cell death was revealed by Annexin V-

FITC/propidium iodide staining. Briefly, cells were washed and incubated for 10 min. in buffer (10 mM HEPES pH7.4, 140mM NaCl, 2.5mM CaCl₂) containing 0.6µg/ml Annexin-V followed by 1.6µg/µl propidium iodide. The number of dead cells was determined by flow cytometry using a FACS caliber cytometer (BD Biosciences, Le Pont de Claix Cedex, France) and the data were analyzed using FlowJo Software (BD Biosciences, Le Pont de Claix Cedex, France) (n=5).

2.7 Animals

in vivo efficacy experiments were carried out on six to seven-week-old female C57BL/6J mice purchased from Janvier (France, Saint Berthevin Cedex, France). The mice were maintained under pathogen-free conditions, and the experiments were carried out in accordance with French laws and regulations. The procedure (number CEEA-2012-148) was approved by the French Ethics Committee for animal experimentation number 6.

2.7.1 *in vivo* antitumor efficacy and Overall Survival (OS) study

in vivo anticancer activity was evaluated against GL261 tumor-bearing C57BL/6J mice. The tumor cell line was detached with trypsin EDTA, washed twice with PBS, counted, and re-suspended to the final concentration desired.

Brain tumors were induced by the stereotaxic inoculation of glioma cells as previously described (Lemaire L, 2000). Briefly, C57BL/6J mice were anesthetized with a mixture of 1µg/g xylazine (Rompun®, Bayer AG, Leverkusen, Germany) and 10µg/g kétamine (Clorketam®, Vétquinol, Lure, France) before being fixed in a stereotactic holder (Stoelting, Dublin, Ireland). Through a small hole drilled in the skull (anterior -0.5mm, lateral 2mm, depth -2.5mm according to the bregma), 3µl of a suspension of 10,000 murine GL261 glioma cells were injected over a 6-min. time period into the caudate putamen of the right hemisphere. The syringe was held in place for an additional minute and was slowly removed to avoid back-filling of the solution.

Twelve days after cell implantation, mice (7-10 mice per group) were intratumorally administered with 10µl of saline, Taxol®, blank LNC, PTX-loaded LNC, PTX-loaded CS-LNC, PTX-loaded LNC plus a separate injection of CpG and M-LNC by Convection Enhanced Delivery (CED) (0.5µl/min).

Animals were observed daily and reduced mobility and significant weight loss (20%) were considered as the limit point for survival curves.

2.7.2 Assessment of tumor evolution by magnetic resonance imaging (MRI)

Prior to therapy, i.e. Day 10 post GL261 inoculation, the mice were scanned using a Bruker Biospec 70/20 operating at a magnetic field of 7T (Bruker, Wissembourg, France) equipped with a ^1H cryoprobe under isoflurane anesthesia (1.5–0.5%, O_2 0.5l/min) to assess tumor development. Mouse body temperature was maintained at 36.5–37.5°C by using a feedback-regulated heating pad during the entire imaging protocol. Anatomical proton images were obtained using a gradient echo sequence (TR = 110ms; echo time (TE) = 3.3ms; $\alpha = 60^\circ$, FOV = 2 * 2cm; matrix 192 * 192; 9-11 contiguous slices of 0.5mm, Nex = 4) after i.v. injection of 10 μl of DOTAREM® (Guerbet, Roissy, France).

On these images, contrast-enhanced regions were manually drawn and the measured area on each slice were multiplied by the slice thickness in order to calculate the entire tumor volume (n=5 for the control and n=3 for the treated animals).

MRI examinations were carried out twice again, on Days 17 and 23 post-inoculation in order to evaluate tumor growth and therefore therapeutic efficiency.

3. Statistical analysis

In the present study, a multifactorial experimental design was employed for process optimization. The effect of the independent variables as SDS and CS concentration on the dependent variables size and zeta potential of the nanoparticles was evaluated. The number of levels used was of 5 as represented in the Table 1. 25 runs were performed in triplicate, which also included the central point.

Cell data (expressed as mean \pm SEM) were analyzed using GraphPad Prism 5.0 software (GraphPad Software, Inc., San Diego, CA, USA). Animal survival data were analyzed using the Kaplan and Meier survival analysis. Statistical analysis used the log-rank test for survival curves and P values of less than 0.05 were considered significant.

4. Results

4.1 Development and characterization of blank and PTX-loaded CS-LNC

Blank and PTX-loaded LNC were successfully obtained following the phase-inversion technique. SDS was used to obtain a negative surface charge on the LNC, necessary for the deposition of CS. SDS was located at the interphase between the oil core and the external aqueous environment and interacts electrostatically with CS, allowing the formation of CS-coated LNCs. CS-SDS interaction was conducted by a combination of electrostatic ion-dipole and hydrophobic interactions that occur when the surfactant is below its critical micelle concentration (CMC=8mM) (Thongngam and McClements, 2004). Figure 1 shows a representation of LNCs modified with SDS and CS.

Pilot experiments were performed to define the optimal production conditions of CS-coated LNC. Briefly, using a multifactorial experimental design, we studied the influence of the SDS and CS concentrations, and their interactions, by varying the amount of both components in the formulation. The studied concentration ranges were from 0 to 4mM and from 0 to 5mg/ml of SDS and CS, respectively.

The analysis of the physico-chemical properties of the LNC showed that all the formulations obtained were of nanometric size, between 50 and 80nm, with zeta potentials indicative of their coating (Figs. 2A and B). SDS, tested at concentrations between 1 and 4mM, did not significantly affect ($p>0.05$) the size of the LNC. However, once the LNC were incubated with CS, there was a logarithmic increase in particle size. Finally, the size reached a plateau which suggests that the particle surface was saturated, and that the excess chitosan did not affect the structure of the system, remaining dissolved into the aqueous medium. The same occurs with the surface charge. In fact, when the surface charge was saturated, any additional CS went into the aqueous phase and did not affect the system.

Using the model to minimize the particle size into the evaluated range, the following conditions were selected in order to obtain particles around 70nm: SDS concentration 4mM and CS concentration 2.5mg/ml.

To achieve the incorporation of PTX into the LNC, SDS-modified or CS-LNC, a given amount of the drug was dissolved into the oily phase of the formulation, followed by the phase inversion and the coating processes. The percentage of the encapsulated drug, in reference to the total amount of drug

dissolved, was very high, up to 98 %, without any influence from the presence of either SDS or CS as compared to the simple LNC (Table 2).

4.2 Stability of PTX-loaded CS-LNC

The stability of coated and uncoated PTX-loaded LNC was assessed upon storage at 4°C for up to 4 weeks. The parameters determined at different time points were: physico-chemical properties, PTX release and stability. No changes in the particle size and zeta potential were observed which confirm that the surface charge of the nanocarriers did not change over time, another indication of chemical and physico-chemical stability of the system. Moreover, no leakage of the drug was shown during the whole experimental period, thus confirming that PTX remains encapsulated into the oily core of the system.

4.3 CpG association to PTX-loaded CS-LNC

Once the base of our multifunctional LNC was optimized, we proceeded to load the CpG on their surface by simple incubation. The formation of complexes between CpG and CS-coated LNC was confirmed by gel-retardation assay. As CpG interacted with CS-coated LNC, via electrostatic interactions, the migration of CpG on agarose gel was retarded due to charge neutralization and to the high molecular weight of the formed complex (Lozano et al., 2013). As shown in Figure 3, no migration of CpG molecules was observed, after its association with the CS-LNC, for theoretical loadings of 0.8-0.75-0.5-0.25% w/w of CpG/CS-coated LNC. To verify the reversibility of the CpG association to nanocapsules, we evaluated the displacement of CpG molecules from the LNC surface by challenging them, using competitive anions such as heparin. For this, an excess of heparin was incubated with CpG-associated LNC. The appearance of the band after heparin treatment illustrates the detachment of CpG molecules from the shell of the nanocapsules. Based on these results, and on the improved stability at 4°C of 0.75% w/w loaded nanocapsules with the respect to the 0.8% formulation, the first one was selected for further studies. The physico-chemical characteristics of the final M-LNC system were the same that the ones obtained for the CS coated PTX-loaded LNC (75nm, 0.2 PI and + 27 mV).

4.4 Induced apoptotic cell death following the treatment with blank and PTX-loaded CS-LNC

GL261 glioblastoma cells were used to study cell apoptosis induced by various PTX formulations. At the earlier events of apoptosis, the membrane protein phosphatidylserine (PS) translocates from the inner side of the plasma membrane to the surface and can be detected by AnnexinV-FITC staining. In later stages of apoptosis, PI can permeate the cell membrane and pass into the nucleus where it binds to the DNA. Then, a double staining AnnexinV-FITC/PI indicates that cells are in a late stage of apoptotic death.

As a first control, GL261 cells were treated with free CpG for 24h to stimulate TLR9 mRNA. As expected, no TLR9 mRNA was detected, as TLR9 receptors were essentially absent in this cell line (Grauer et al., 2008). In contrast, TLR9 mRNA was found in the central nervous system homogenate (which contains all the immunological cells) used as a positive control.

GL261 cell death induction after 24h treatment with BCNU (500 μ M) used as another positive control was evaluated. In fact, BCNU induced strong cell death: 20% of GL261 cells in the early apoptotic phase (Ann⁺ / P.I) and 80% in the late apoptotic phase (Ann⁺ / P.I⁺).

The number of GL261 cells undergoing apoptosis was evaluated following different treatments with: PTX ethanol solution, PTX-loaded CS-LNC, and the respective blank systems (Figure 4).

At 7 and 10 μ M, PTX ethanol solution induces a high proportion of late apoptotic cells with 73% and 70%, respectively. When CS-LNC were used to encapsulate PTX, about 50% of the cells experienced late apoptotic cell death. Blank LNC and blank CS-coated LNC, tested at the same concentration of drug-loaded LNC, induced a low apoptotic cell death with 10% of late apoptotic cells at an LNC concentration of 0.621mg/ml. This effect could be related to a different mechanism of LNC uptake. In fact, as already demonstrated for PTX-loaded LNC, the encapsulation of the drug into the LNC did not lead to an increase of PTX uptake in GL261 glioma cells. Balzeau *et al.* demonstrated that only through the functionalization of the LNC could the cell uptake be improved [17]. Finally, M-LNC were tested and, due to the absence of TLR9 receptors on GL261, the same apoptotic behavior of PTX-loaded CS-LNC was observed.

4.5 *in vivo* study

The *in vivo* antitumor efficacy of the M-LNC was evaluated in a GL261 glioma mouse model. The OS study was carried out by grouping the animals into seven different treatment, formulation and schedule times (Figure 5). On Day 0, GL261 cells were implanted into the brain of the animals, and the treatment was carried out 12 days later. On Days 10, 17 and 23 after cell implantation, tumor volumes were assessed using MRI. The OS curves were analyzed according to Kaplan-Meier method and compared using a log-rank test. As shown in Figure 6, when mice were treated with PTX-loaded LNC, PTX-loaded LNC plus a separate injection of CpG solution, or PTX-loaded CS-LNC the median of survival did not differ from the control animals receiving saline solution (Table 3). However, treatment with M-LNC significantly increased the mouse median survival time (34 days) compared to the saline group (28 days). This result shows that the co-administration in the same system of the cytotoxic agent PTX, and the immunoadjuvant CpG, affected the OS of the animals.

4.6 Monitoring of tumor growth by magnetic resonance imaging

Alongside the OS study, MRI investigation was carried out to better characterize therapy efficiency, especially in the M-LNC group, which gave the best results in terms of OS and median of survival as compared to the control saline group.

First of all, due to the low natural contrast between GL261 brain tumor and brain parenchyma, both on T1- and T2-weighted images, administration of the MR contrast agent was compulsory to delineate the brain tumor (Figure 7). The stereotactic injection of saline did not restrain tumor development which was of about 10 μ l on Day 10, and reached 15 μ l on Day 17 and 83 μ l on Day 23 (Figure 8). However, treatment with M-LNC significantly impaired tumor growth with a reduction in size of 50% by Day 23.

5. Discussion

With the purpose of taking advantage of the synergistic effect between chemo and immunotherapy, the goal of the present study was the development of a multifunctional nanosystem capable of delivering the anticancer drug PTX, simultaneously with the immunostimulating CpG into brain tumors.

Despite its promises, the clinical utility of free CpG still faces several challenges which limit its effectiveness. The development of nanosystems for the *in vivo* delivery of CpG has successfully addressed a number of these shortcomings by providing an efficient means to improve pK characteristics, to protect it from degradation and provide a direct transport to target cells. Lipid-based nanoparticles have been shown to exert improved immunotherapeutic activity of CpG into TLR9-rich endosomes *in vitro* and *in vivo* in different tumor models (Chikh et al., 2009; Wilson et al., 2009). Also, the ability of nanosystems to enhance the activity of CpG as an immune response modifier is of particular relevance and has been previously described (Ursu and Carpentier, 2012).

All these effective preclinical and even early clinical strategies have not been translated into successful human therapies, which have questioned the clinical utility of free and/or encapsulated CpG. From here, the rationale of our multifunctional nanosystem designed to combine the action of CpG and the cytotoxic drug PTX was set. We demonstrated that functionalized LNC loaded with both PTX and CpG could be used to synergize the chemo-immuno response leading to an improvement of the overall therapeutic activity.

With this aim, suitable PTX-loaded LNCs were modified with a cationic polymeric coating. This structure was expected to have a double role: the lipidic core of the LNC would allow an improvement of hydrophobic drug bioavailability and stability, and the external coating would confer immunostimulant properties through the presence of CpG. CS was selected as a natural biopolymer to provide a positive charge layer around the oil droplets after immobilization by layer by layer deposition (Démoulin, T., 2014). The biophysical properties of chitosan–genetic material complexes and their capacity for transfection have been investigated in detail and beneficial properties include a low molecular weight, a high DD (Degree of DeAcetylation), a small particle size (100 nm), and a moderate positive surface zeta potential along with a high (+/-) charge ratio (Santos-Carballal B. 2015; and Démoulin, T. 2014). In this work, low Mw (kDa) CS with a high DD was chosen to coat the LNC. The rationale behind this choice was that i) high DD chitosan results in an increased positive charge and water solubility, thus enabling a greater CpG binding capacity (Démoulin et al., 2014; Agirre M. 2014), and ii) low MW chitosan has been associated with minor cytotoxicity compared to high MW polymers (Alameh M, 2012; Liu et al., 2007).

The novel multifunctional nanocarrier made of CS-LNC was developed. The addition of the polycationic CS induces a slight increase in size (from 55nm to 70nm) but a major change in surface charge (from -6mV for uncoated LNC to +30mV in CS-coated LNC) allowing the layer deposition of CpG. Moreover, the incubation of CpG did not modify the physico-chemical characteristics of the system, the size was in an appropriate range (70nm), and no variation in zeta potential and no leakage of PTX were observed. This improved the stability of the drug-loaded nanosystems, together with the ability to associate CpG on the surface, making the carrier suitable for further interaction with the TLR 9-receptor expressed in microglia cells (Rivest, 2009).

In the first set of experiments, we evaluated the relative distribution of early apoptotic and late apoptotic/necrotic cells following treatment with blank and PTX-loaded LNC (Figure 3). In our study we showed that blank LNC or CS-LNC did not induce any apoptotic effect. On the contrary, due to the high sensitivity of these cells to the drug, PTX solution induced a considerable apoptotic effect. The greatest effect was obtained with PTX-loaded CS-LNCs, with a value of late apoptotic cells of about 50%. This effect could probably be explained by a different mechanism of internalization of the modified LNC that deserves further investigation.

Then, the *in vivo* antitumor activity of the different treatments was evaluated in the GL261 tumor mice model. The GL261 glioma model, which is the gold standard syngeneic model for screening pre-clinical treatments in glioma, is fully relevant since it is a highly reproducible and easy-to-establish model system and does not compromise the immune response (Maes and Van Gool, 2011). In our study, the intracranial injection of M-LNCs, enhanced the antitumor effect of drug-loaded LNC or CpG alone.

According to Jarry *et al.*, intratumor injection of free CpG has poor efficiency in inducing tumor regression, which is in agreement with clinical trials in recurrent malignant glioma showing low therapeutic efficacy of intracerebral CpG administration (Jarry *et al.*, 2014). The same occurred with Taxol®, the commercial formulation of paclitaxel, and with the administration of PTX-loaded LNC and CpG separately, evidencing that only from a combined approach could the treatment be effective. The results of the OS shown in Figure 6 demonstrate the therapeutic effect evoked by the administration of a single system that could allocate PTX and the immunostimulant agent. The

immunotherapeutic and synergistic effect resulting from the association of PTX and CpG could be ascribed to different factors. Firstly, GL261 tumor cells do not express TLR9, and hence the therapeutic effect observed in the OS study could be attributed to the direct stimulation of microglia cells (Grauer et al., 2008). Secondly, as reported in the literature, PTX antitumor activity causes direct cell death which leads to the release of tumor-specific antigens from tumor cells as well as danger signals – damage-associated molecular patterns (DAMPs). All these events contribute to the stimulation and the recruitment of immunocompetent cells (Roy et al., 2013; Szajnik et al., 2009). Our findings have direct implications on the development of CNS-based treatment for malignant brain tumors. The strategy based on a single *in situ* administration of both CpG and PTX, can be employed to overcome a local immunosuppressive microenvironment through modulations of tumor immune response.

6. Conclusions

In this work, we report the design of a novel multifunctional carrier based on the incorporation of a cytotoxic drug, PTX, and a TLR9 receptor agonist, CpG, on CS-modified LNC and their use in a chemo-immunotherapy strategy. CS-coated nanocarriers exhibited attractive properties for the encapsulation and delivery of both anticancer drug and genetic material. The co-administration of CpG and PTX with the same nanocarrier in the orthotopic GL261 glioma mouse model significantly improved the survival rate of the animals as compared with Taxol[®] and the separate administration of PXT-loaded nanocapsules and CpG. Consequently, this strategy could be of interest for achieving an antitumor effect through stimulation of the immune system. Combining chemotherapy with innovative immunotherapy, in the GL261 system, will lead to a novel chemo-immunotherapeutic approach to control the long-term disease and hopefully induce tumor rejection.

Acknowledgments

This work was supported by the Region Pays de la Loire (France) Project: CIMATH2. The authors would like to thank the technicians from ‘Service Commun Animalerie Hospitalo-Universitaire d’Angers’ (SCAHU) for the housing and care of the animals used in this study. We also thank Karim Bey who contributed to the development of the *in vitro* studies.

References

- Alameh M, D.D., Jean M, Darras V, Thibault M, Lavertu M, Buschmann MD, Merzouki A., 2012. Low molecular weight chitosan nanoparticulate system at low N:P ratio for nontoxic polynucleotide delivery. *Int J Nanomedicine*. 7, 1399-1414.
- Agirre M., Zarate J., Ojeda E., Puras G., Desbrieres J. and Pedraz JL. 2014. Low Molecular Weight Chitosan (LMWC)-based Polyplexes for pDNA Delivery: From Bench to Bedside. 6, 1727-1755.
- Andaloussi, A.E., Sonabend, A.M., Han, Y., Lesniak, M.S., 2006. Stimulation of TLR9 with CpG ODN enhances apoptosis of glioma and prolongs the survival of mice with experimental brain tumors. *Glia* 54, 526-535.
- Badie B, Berlin JM., 2013. The future of CpG immunotherapy in cancer. *Immunotherapy* 5, 1-3.
- Balzeau, J., Pinier, M., Berges, R., Saulnier, P., Benoit, J.-P., Eyer, J., 2013. The effect of functionalizing lipid nanocapsules with NFL-TBS.40-63 peptide on their uptake by glioblastoma cells. *Biomaterials* 34, 3381-3389.
- Buchanan, M.M., Hutchinson, M., Watkins, L.R., Yin, H., 2010. Toll-like receptor 4 in CNS pathologies. *Journal of Neurochemistry* 114, 13-27.
- Carpentier, A., Metellus, P., Ursu, R., Zohar, S., Lafitte, F., Barrié, M., Meng, Y., Richard, M., Parizot, C., Laigle-Donadey, F., Gorochoy, G., Psimaras, D., Sanson, M., Tibi, A., Chinot, O., Carpentier, A.F., 2010. Intracerebral administration of CpG oligonucleotide for patients with recurrent glioblastoma: a phase II study. *Neuro-Oncology* 12, 401-408.
- Carter M Suryadevara, T.V., Luis Sanchez-Perez, Elizabeth A Reap, Bryan D Choi, Peter E Fecci, John H Sampson, 2015. Immunotherapy for malignant glioma. *Surg Neurol Int* 6.
- Chatterjee, S., Salaün, F., Campagne, C., Vaupre, S., Beirão, A., 2012. Preparation of microcapsules with multi-layers structure stabilized by chitosan and sodium dodecyl sulfate. *Carbohydrate Polymers* 90, 967-975.
- Chikh, G., de Jong, S.D., Sekirov, L., Raney, S.G., Kazem, M., Wilson, K.D., Cullis, P.R., Dutz, J.P., Tam, Y.K., 2009. Synthetic methylated CpG ODNs are potent in vivo adjuvants when delivered in liposomal nanoparticles. *International Immunology* 21, 757-767.
- Démoulin, T., Milona, P., McCullough, K.C., 2014. Alginate-coated chitosan nanogels differentially modulate class-A and class-B CpG-ODN targeting of dendritic cells and intracellular delivery. *Nanomedicine: Nanotechnology, Biology and Medicine* 10, 1739-1749.
- Finocchiaro, G., Pellegatta, S., 2011. Immunotherapy for glioma: getting closer to the clinical arena? *Current Opinion in Neurology* 24, 641-647.
- Finocchiaro G, P.S., 2014. Perspectives for immunotherapy in glioblastoma treatment. *Curr Opin Oncol*. 26, 608-614.
- Garcion, E., Lamprecht, A., Heurtault, B., Paillard, A., Aubert-Pouessel, A., Denizot, B., Menei, P., Benoit, J.-P., 2006. A new generation of anticancer, drug-loaded, colloidal vectors reverses multidrug resistance in glioma and reduces tumor progression in rats. *Molecular Cancer Therapeutics* 5, 1710-1722.
- Grauer, O., Pöschl, P., Lohmeier, A., Adema, G., Bogdahn, U., 2007. Toll-like receptor triggered dendritic cell maturation and IL-12 secretion are necessary to overcome T-cell inhibition by glioma-associated TGF- β 2. *Journal of Neuro-Oncology* 82, 151-161.
- Grauer, O.M., Molling, J.W., Bennink, E., Toonen, L.W.J., Suttmüller, R.P.M., Nierkens, S., Adema, G.J., 2008. TLR Ligands in the Local Treatment of Established Intracerebral Murine Gliomas. *The Journal of Immunology* 181, 6720-6729.
- Groo AC, S.P., Gimel JC, Gravier J, Ailhas C, Benoit JP, Lagarce F, 2013. Fate of paclitaxel lipid nanocapsules in intestinal mucus in view of their oral delivery. *Int J Nanomedicine*. 8, 4291-4230.
- Heurtault B, S.P., Pech B, Proust JE, Benoit JP., 2002. A novel phase inversion-based process for the preparation of lipid nanocarriers. *Pharmaceutical Research* 19, 875-880.
- Jarry, U., Donnou, S., Vincent, M., Jeannin, P., Pineau, L., Fremaux, I., Delneste, Y., Couez, D., 2014. Treg depletion followed by intracerebral CpG-ODN injection induce brain tumor rejection. *Journal of Neuroimmunology* 267, 35-42.
- Javeed, A., Ashraf, M., Riaz, A., Ghafoor, A., Afzal, S., Mukhtar, M.M., 2009. Paclitaxel and immune system. *European Journal of Pharmaceutical Sciences* 38, 283-290.

- Lemaire L, F.F., Saint-Andre JP, Roullin VG, Jallet P, Le Jeune JJ., 2000. High-field quantitative transverse relaxation time, magnetization transfer and apparent water diffusion in experimental rat brain tumour. *NMR Biomed* 13, 116-123.
- Liu, X., Howard, K.A., Dong, M., Andersen, M.Ø., Rahbek, U.L., Johnsen, M.G., Hansen, O.C., Besenbacher, F., Kjems, J., 2007. The influence of polymeric properties on chitosan/siRNA nanoparticle formulation and gene silencing. *Biomaterials* 28, 1280-1288.
- Lozano, M.V., Lollo, G., Alonso-Nocelo, M., Brea, J., Vidal, A., Torres, D., Alonso, M.J., 2013. Polyarginine nanocapsules: a new platform for intracellular drug delivery. *Journal of Nanoparticle Research* 15, 1-14.
- Maes, W., Van Gool, S., 2011. Experimental immunotherapy for malignant glioma: lessons from two decades of research in the GL261 model. *Cancer Immunology, Immunotherapy* 60, 153-160.
- Reardon, D.A., Wucherpennig, K.W., Freeman, G., Wu, C.J., Chiocca, E.A., Wen, P.Y., Curry, W.T., Mitchell, D.A., Fecci, P.E., Sampson, J.H., Dranoff, G., 2013. An update on vaccine therapy and other immunotherapeutic approaches for glioblastoma. *Expert Review of Vaccines* 12, 597-615.
- Rivest, S., 2009. Regulation of innate immune responses in the brain. *Nat Rev Immunol* 9, 429-439.
- Roy, A., Singh, M.S., Upadhyay, P., Bhaskar, S., 2013. Nanoparticle mediated co-delivery of paclitaxel and a TLR-4 agonist results in tumor regression and enhanced immune response in the tumor microenvironment of a mouse model. *International Journal of Pharmaceutics* 445, 171-180.
- Santos-Carballal B., Aldering LJ., Ritzefeld M., Pereira S., Sewald N., Moerschbacher BM., Götte M., Goycoolea FM. 2015. Physicochemical and biological characterization of chitosan-microRNA nanocomplexes for gene delivery to MCF-7 breast cancer cells. *Scientific Reports* 5, 13567.
- Szajnik, M., Szczepanski, M.J., Czystowska, M., Elishaev, E., Mandapathil, M., Nowak-Markwitz, E., Spaczynski, M., Whiteside, T.L., 2009. TLR4 signaling induced by lipopolysaccharide or paclitaxel regulates tumor survival and chemoresistance in ovarian cancer. *Oncogene* 28, 4353-4363.
- Thongngam, M., McClements, D.J., 2004. Characterization of Interactions between Chitosan and an Anionic Surfactant. *Journal of Agricultural and Food Chemistry* 52, 987-991.
- Ursu, R., Carpentier, A., 2012. Immunotherapeutic Approach with Oligodeoxynucleotides Containing CpG Motifs (CpG-ODN) in Malignant Glioma, in: Yamanaka, R. (Ed.), *Glioma*. Springer New York, pp. 95-108.
- Vicente, S., Peleteiro, M., Gonzalez-Aramundiz, J.V., Díaz-Freitas, B., Martínez-Pulgarín, S., Neissa, J.I., Escribano, J.M., Sanchez, A., González-Fernández, Á., Alonso, M.J., 2014. Highly versatile immunostimulating nanocapsules for specific immune potentiation. *Nanomedicine*, 1-17.
- Wilson, K.D., de Jong, S.D., Tam, Y.K., 2009. Lipid-based delivery of CpG oligonucleotides enhances immunotherapeutic efficacy. *Advanced Drug Delivery Reviews* 61, 233-242.
- Zitvogel, L., Apetoh, L., Ghiringhelli, F., Kroemer, G., 2008. Immunological aspects of cancer chemotherapy. *Nat Rev Immunol* 8, 59-73.

Figure Captions

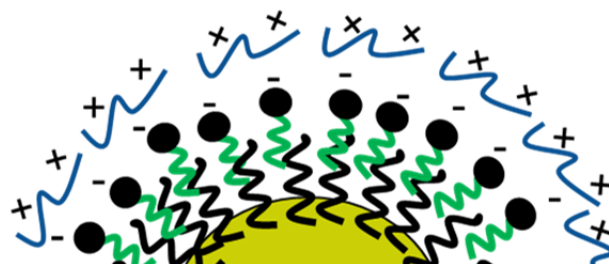


Figure 1: Schematic representation of LNC prepared with SDS and CS.

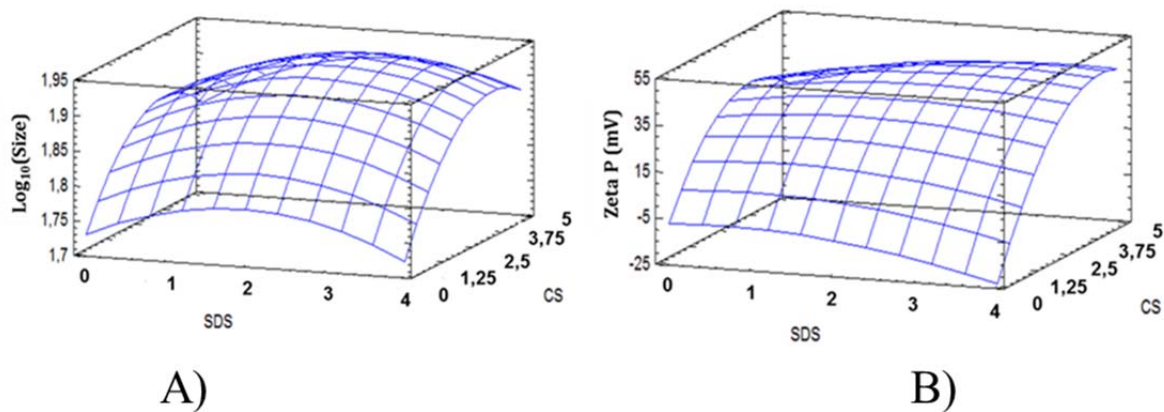


Figure 2: A) Response surface showing the effect of SDS concentration (mM) and CS (mg/ml) on the particle size of blank LNC. B) Response surface showing the effect of SDS concentration (mM) and CS (mg/ml) on the surface charge of blank LNC.

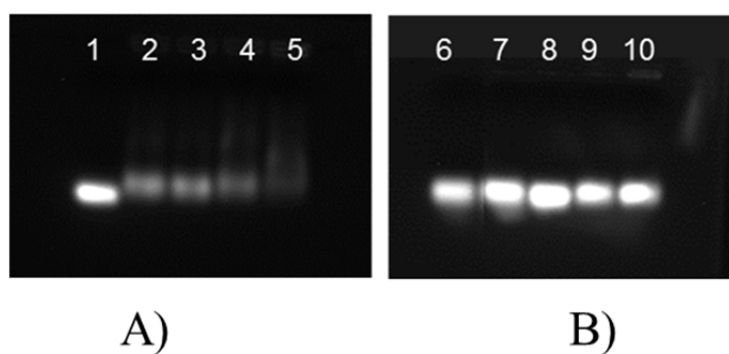


Figure 3: (A) Agarose gel electrophoresis retardation assay of CpG interacting with CS-LNC at different CpG/CS ratios. B) Release assay. CpG was released by adding an excess of heparin (15mg/ml) to the suspension prepared at different CpG ratios.

1-naked CpG, 2-0.8% w/w CpG associated PTX-loaded CS-LNC, 3-0.75% w/w CpG associated PTX-loaded CS-LNC, 4-0.5% w/w CpG associated PTX-loaded CS-LNC, 5-0.25% w/w CpG associated PTX-loaded CS-LNC. 6-7-8-9-10 represents the wells 1-2-3-4-5 incubated with the excess heparin.

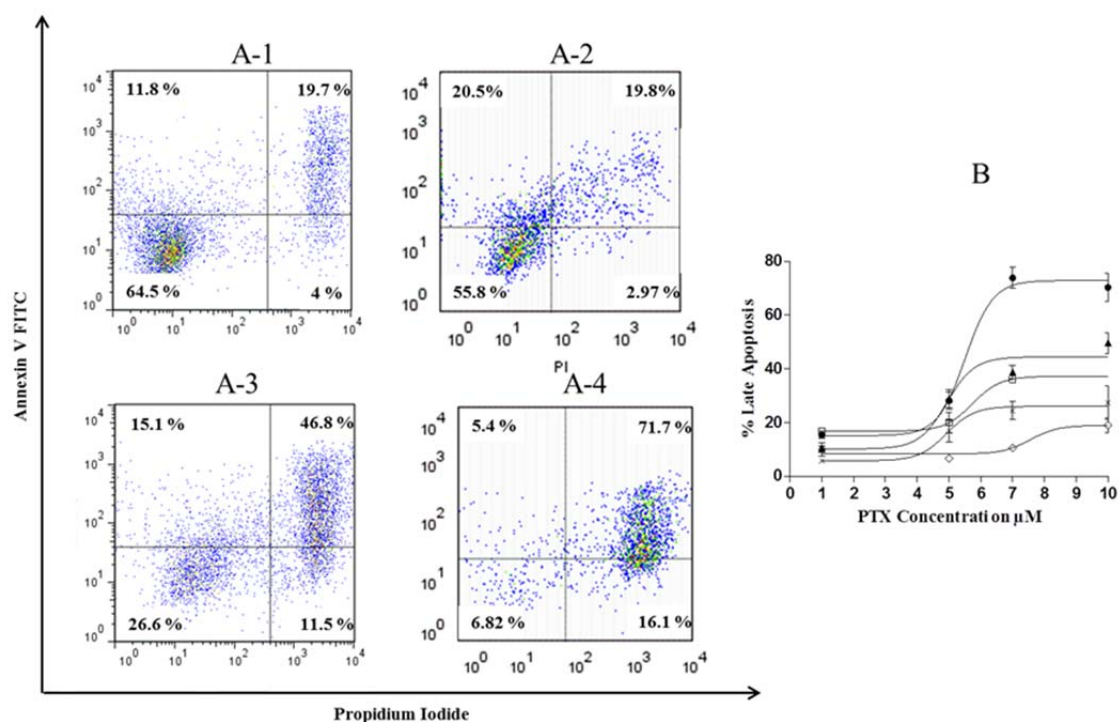


Figure 4: The apoptosis study of GL 261 cells after 24 hours of incubation with 0.6mg/ml of blank LNC (A-1) and blank CS-LNC (A-2), PTX-loaded CS-LNC at PTX concentration of 7 μ M (A-3), PTX ethanol solution at PTX concentration of 7 μ M (A-4). B: Cells incubated for 24h with various concentrations of PTX Ethanol solution (●), Blank LNC (◇), PTX-loaded CS-LNC (▲), blank CS-LNC (X) and CpG-PTX-loaded CS-LNC (□) (n = 3, mean \pm SEM).

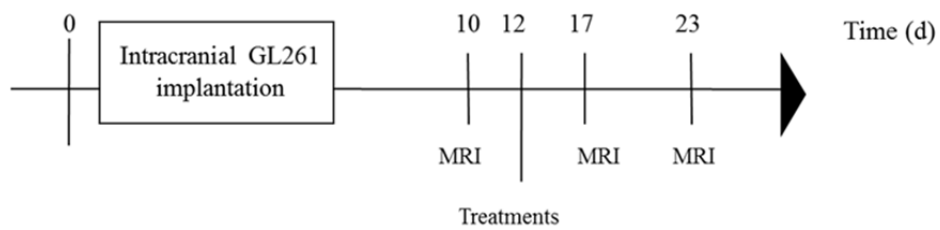


Figure 5: Schedule of administration established to perform the OS study. On Day 0 GL261 cells were implanted. Then, on Day 12 the different treatments were administered through CED. On Days 10, 17 and 23, MRI images of mice treated with saline and M-LNC were taken to follow tumor evolution

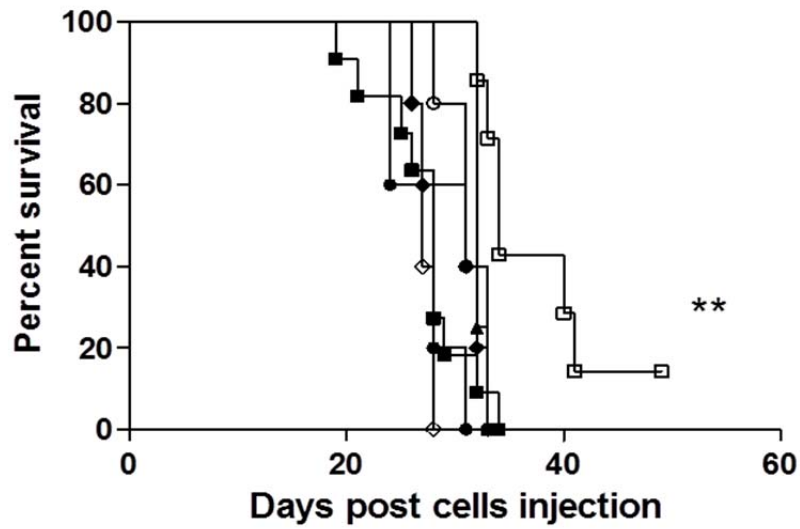


Figure 6: Evolution of mouse survival following stereotactic injection by CED of 10 μ l of blank LNC (◇), PTX-loaded LNCs (■), PTX-loaded LNC + CpG (●), PTX-loaded CS-LNC (▲), and M-LNC (□). Taxol® and saline solutions were used as controls. Log-rank (Mantel Cox) test: **, p value = 0.0014. n = 7-10 mice per group.

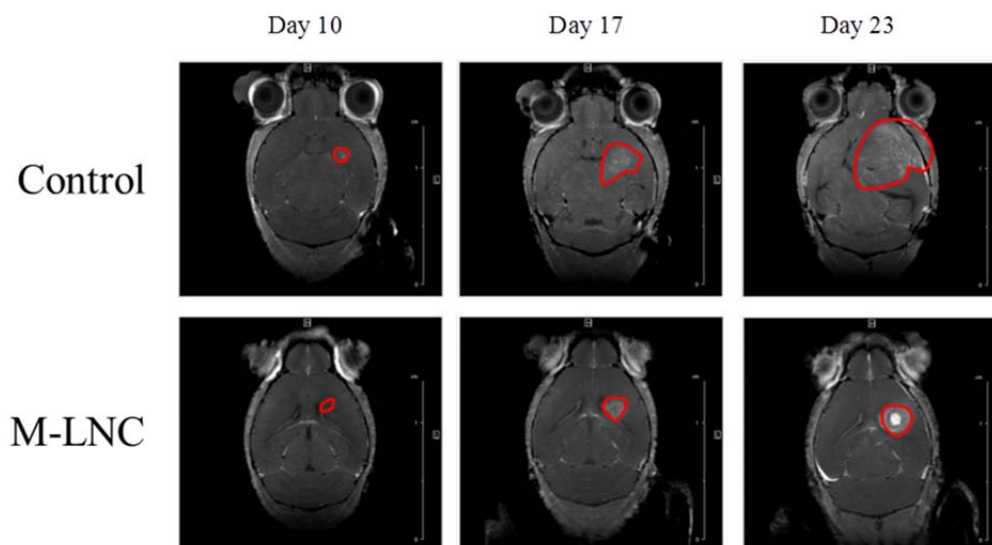


Figure 7: T1-weighted images of GL261-bearing mice after IV injection of Dotarem®. Frames A correspond to saline solution-treated mice imaged on Days 10, 17 and 23 after cell inoculation. Frames B correspond to M-LNC-treated mice imaged on Days 10, 17 and 23 after cell inoculation.

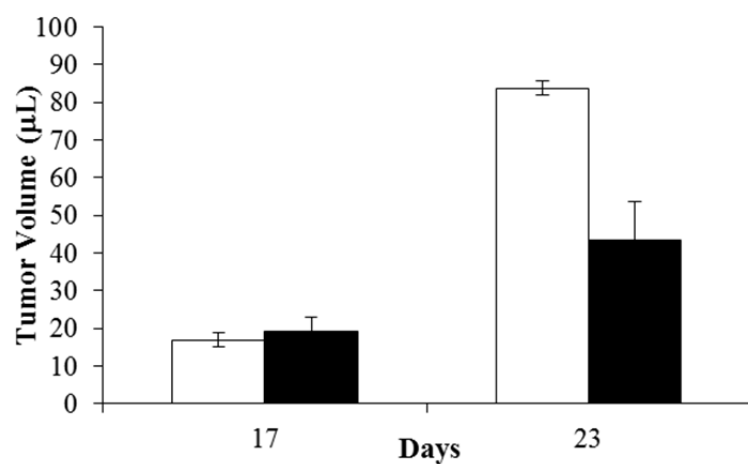


Figure8: Measurement of tumor volume evolution following stereotactic injection by CED of 10μl, Saline (□) and M-LNC (■). Data represent $n=3 \pm \text{SME}$ (90% confidence interval).

Tables

Table 1: Independent variables and their levels for the multifactorial experimental design. CS: chitosan and SDS: Sodium dodecyl sulphate.

Symbol	Units	-1 Level	-0.5 Level	0 Level	+0.5 Level	+1 Level
CS	mg/ml	0	1.25	2.5	3.75	5
SDS	mM	0	1	2	3	4

Table 2. Characteristics of three different formulations following the optimized conditions calculated from the multifactorial experimental design. n= 3.

Formulation	SDS (mM)	CS (mg/ml)	Size (nm)	PI	Zeta Potential (mV)	% Drug detected
PTX-loaded LNC	-	-	55.4± 1.5	< 0.1	-6.5±1.8	98
PTX-loaded LNC-SDS	4mM	-	53.1±1.5	< 0.1	-22.9±1.2	98
PTX-loaded CS-LNC	4mM	2.5	69.9± 3.4	0.19	+30.8±5.9	98

Table 3: Summary of the median survival of mice after GL261 implantation and treatment.

Treatment	Median Survival (day)
Control	28
Blank LNC	27
Taxol®	28
PTX-Loaded LNC	31
PTX-Loaded LNC + CpG	31
PTX-Loaded CS-LNC	31
M-LNC	34**